Magnetic excitations in an ionic spin-chain system with a nonmagnetic ferroelectric instability

K. Sunami,[1,*] Y. Sakai,[1] R. Takehara,[1] H. Adachi,[1] K. Miyagawa,[1] S. Horiuchi,[2] and K. Kanoda[1,†]

[1]*Department of Applied Physics, University of Tokyo, Bunkyo-ku, Tokyo 113-8656, Japan*

[2]*Research Institute for Advanced Electronics and Photonics (RIAEP), National Institute of Advanced Industrial Science and Technology (AIST), Tsukuba, Ibaraki 305-8565, Japan*

(Received 25 September 2020; revised 12 November 2020; accepted 13 November 2020; published 7 December 2020)

Cross-correlation between magnetism and dielectric is expected to offer distinct emergent phenomena. Here, magnetic excitations in the organic donor-acceptor spin-chain system, tetrathiafulvalene-bromanil (TTF-BA), with a ferroelectric ground state is investigated by ^{1}H-NMR spectroscopy. A nonmagnetic transition with a ferroelectric order is marked by sharp drops in the NMR shift and the nuclear spin relaxation rate T_1^{-1} at 53 K. Remarkably, the analyses of the NMR shift and T_1^{-1} dictate that the paramagnetic spin susceptibility in TTF-BA is substantially suppressed from that expected for the one-dimensional Heisenberg spins. We propose that the spin-lattice coupling and the ferroelectric instability cooperate to promote precursory polar singlet formation in the ionic spin system with a nonmagnetic ferroelectric instability.

DOI: 10.1103/PhysRevResearch.2.043333

I. INTRODUCTION

One-dimensional (1D) systems possess coupled electron-lattice instabilities, a metal-insulator (Peierls) transition for itinerant electron systems, and a paramagnetic-nonmagnetic (spin-Peierls) transition for localized spin systems [1,2]. Organic charge-transfer complexes of a quasi-1D nature are representative platforms for the study of these issues. Among them, tetrathiafulvalene-chloranil (TTF-CA) composed of 1D mixed stacks of donor molecules, TTF, and acceptor molecules, CA, is a fascinating material showing a neutral-ionic (NI) transition accompanied by a symmetry-breaking lattice dimerization at 81 K under ambient pressure [3,4]; it switches from a paraelectric neutral phase ($TTF^{+\rho}$-$CA^{-\rho}$ with $\rho \sim 0.3$) to a ferroelectric ionic phase ($\rho \sim 0.6$–0.7). On the other hand, the analogous material, tetrathiafulvalene-bromanil (TTF-BA), in which Cl atoms in CA molecules are substituted by Br atoms [Fig. 1(a)], is in a highly ionic state ($\rho \sim 0.95$) at all temperatures [5] with every molecule accommodating a $S = 1/2$ spin, which is paramagnetic at room temperature. Upon cooling, TTF-BA exhibits a nonmagnetic dimerization transition with ferroelectricity [6,7], putatively a spin-Peierls transition, at 53 K [5].

Recent under-pressure studies of TTF-CA have revealed that the ionic phase above ∼9 kbar is nondimerized and paraelectric around room temperature and undergoes a dimerized ferroelectric transition upon cooling [8,9], evoking a view that TTF-BA is equivalent to TTF-CA under pressures above ∼9 kbar. Notably, it has recently been shown that the magnetism and conductivity in the paraelectric ionic phase of TTF-CA under pressure are attributed to spin and charge solitons [10,11]. As shown in Fig. 1(b), however, the resistivity in TTF-BA (measured in the present study) is 6 to 7 orders of magnitude larger than that in TTF-CA under pressure [12], indicating the absence of charge-soliton excitations in TTF-BA; thus, TTF-BA offers a distinct localized spin system with a polarized nonmagnetic ground state.

The present study aims to reveal the nature of spin excitations in TTF-BA, a polarizable Heisenberg antiferromagnetic spin-chain system with a nonmagnetic ferroelectric transition, by ^{1}H-NMR measurements. In general, ^{1}H-NMR has insufficient sensitivity for probing the electronic state because of small hyperfine coupling and molecular motions unwantedly contributing to the NMR relaxation rate. TTF-BA, however, has sizable ^{1}H hyperfine coupling constants, no motional molecular parts, and, further, appreciably large static and dynamical spin susceptibilities as described later. Owing to all these features of TTF-BA, ^{1}H-NMR is competent for probing the spin states.

II. EXPERIMENTAL

We performed ^{1}H-NMR measurements on a single crystal of TTF-BA under the magnetic field H of 3.7 T applied parallel to the b^* axis (perpendicular to the ac plane). In this field configuration, there are four nonequivalent ^{1}H nuclei above T_c [denoted by $H_\alpha(1)$ and $H_\alpha(2)$ on the α-stack running along the a axis and $H_\beta(1)$ and $H_\beta(2)$ on the β-stack along the b axis in Fig. 1(c)]. To acquire NMR signals, we employed the so-called solid-echo pulse sequence. The origin of the NMR line shift corresponds to the resonance frequency for tetramethylsilane (TMS). The spin-lattice relaxation rate T_1^{-1} was determined by fitting the stretched

*sunami@mdf2.t.u-tokyo.ac.jp
†kanoda@ap.t.u-tokyo.ac.jp

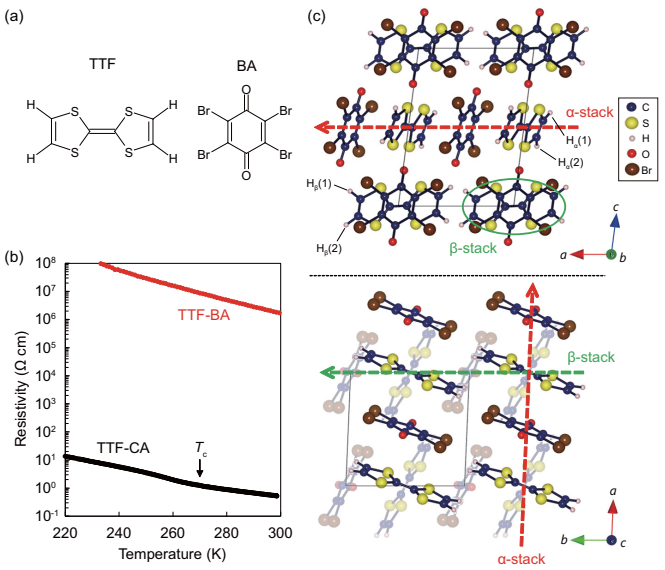

FIG. 1. (a) Molecular structures of TTF and BA. (b) Temperature dependence of electrical resistivity in TTF-BA under 5 kbar (red line) and TTF-CA under 14 kbar [12] (black line) measured by the four-terminal method. The resistance in TTF-BA at ambient pressure is too high ($>10^6$ Ω) to measure by the four-terminal method, and thus we present the 5-kbar data. T_c is the ferroelectric transition temperature in TTF-CA at 14 kbar. (c) Crystal structures of TTF-BA viewed from the *b* (upper) and *c* (lower) axes [7].

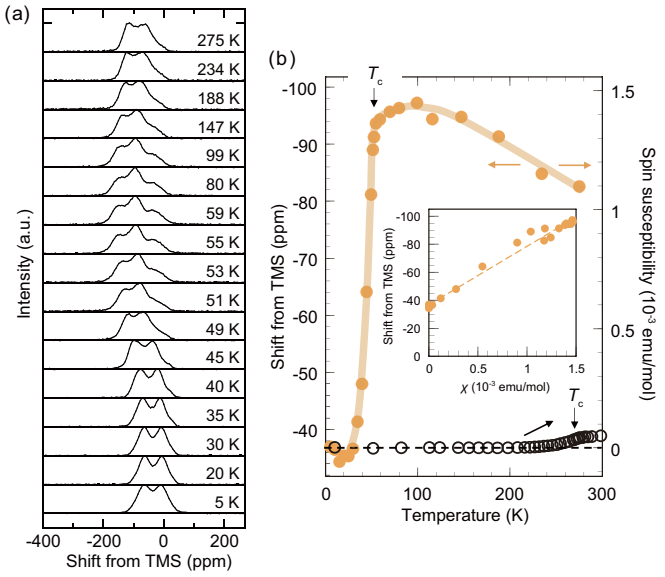

FIG. 2. Temperature profiles of the ^{1}H-NMR spectra (a) and the first moments of spectra in TTF-BA (solid yellow circles) (b). In panel (b), the right axis denotes the scale of the spin susceptibility χ and the open black circles represent χ in TTF-CA under 14 kbar [12]. Inset of panel (b): Plot of spectral shift vs spin susceptibility reported in Ref. [6] in TTF-BA.

exponential function to the relaxation curve of the nuclear magnetization obtained using the standard saturation method. The relaxation curve is nearly single exponential except below the nonmagnetic transition temperature, where a somewhat nonsingle exponential feature appears very probably due to the orphan spins failing to form singlets and/or minor impurity spins as seen later. The frequency dependence of T_1^{-1} was measured in the range of 20–370 MHz, which corresponds to 0.5–8.6 T.

III. RESULTS

A. NMR spectra

^{1}H-NMR spectrum at around room temperature is formed by slightly asymmetric two broad peaks [Fig. 2(a)]. Upon cooling, the spectrum changes its shape but turns into two symmetric peaks below ∼50 K. The spectral shift defined by the first moment of the entire spectrum is plotted in Fig. 2(b); it shows a maximum around ∼100 K and a sharp decrease indicating the nonmagnetic transition at $T_c = 53$ K. The spectral shift is contributed by the spin shift, proportional to the spin susceptibility χ, and the temperature-independent chemical shift. These are separated by plotting the shift values against the previously reported χ values [6] [inset of Fig. 2(b)]; the slope of the linearity gives the hyperfine coupling component parallel to the field direction averaged for the four ^{1}H sites, $a_\parallel^{\rm ave}$, of -0.47 kOe/μ_B, and the intercept determines the chemical shift of -37 ppm, which has an uncertainty of tens of ppm but is not involved in the present analysis.

The hyperfine coupling tensors have anisotropies arising from the dipolar interactions between nuclear and electron spins. We evaluate a dipolar field at each ^{1}H site generated by the electron spin as follows: (i) a magnetic moment of 1 μ_B is distributed over the atomic sites (precisely, nuclear positions) in a molecule according to the Mulliken populations calculated by the extended Hückel method [13] using the atomic coordinates at 293 K reported in Ref. [7], and (ii) we incorporate dipole fields from electron spins on six neighboring molecules. For the present field configuration ($H \parallel b^*$), the dipole hyperfine coupling components parallel to the field direction are calculated to be 0.35, 0.41, -0.22, and -0.32 kOe/μ_B for $H_\alpha(1)$, $H_\alpha(2)$, $H_\beta(1)$, and $H_\beta(2)$, respectively, whose average $(a_\parallel^{\rm aniso})^{\rm ave}$ is 0.05 kOe/μ_B. The observed value of -0.47 kOe/μ_B is contributed by the dipole (anisotropic) part, $(a_\parallel^{\rm aniso})^{\rm ave}$, and an isotropic part, $a^{\rm iso}$, which thus yields -0.52 $(= -0.47 - 0.05)$ kOe/μ_B; this value is a little different from $a^{\rm iso} = -0.39$ kOe/μ_B evaluated in TTF-CuBDT [14]. The isotropic part $a^{\rm iso}$ is determined by the contact interaction from the on-site electron spin at the ^{1}H site and the transferred hyperfine coupling from the electron spin at the adjacent carbon site; the former is negligibly small for the ^{1}H site located on the edges of molecule. For the latter, the spin density at the adjacent carbon site is affected by the surroundings such as the neighboring molecular species and their arrangements, and thus the size of $a^{\rm iso}$ is likely to vary from material to material. The asymmetric shape of spectra above T_c possibly arises from the different anisotropic local fields at the four ^{1}H sites as estimated above. Below T_c, where the spin shift vanishes, the spectra take the shape of the so-called Pake doublet derived from the nuclear dipolar interactions between $H_{\alpha(\beta)}(1)$ and $H_{\alpha(\beta)}(2)$, possibly broadened by the anisotropic chemical shift tensor giving site-dependent shifts.

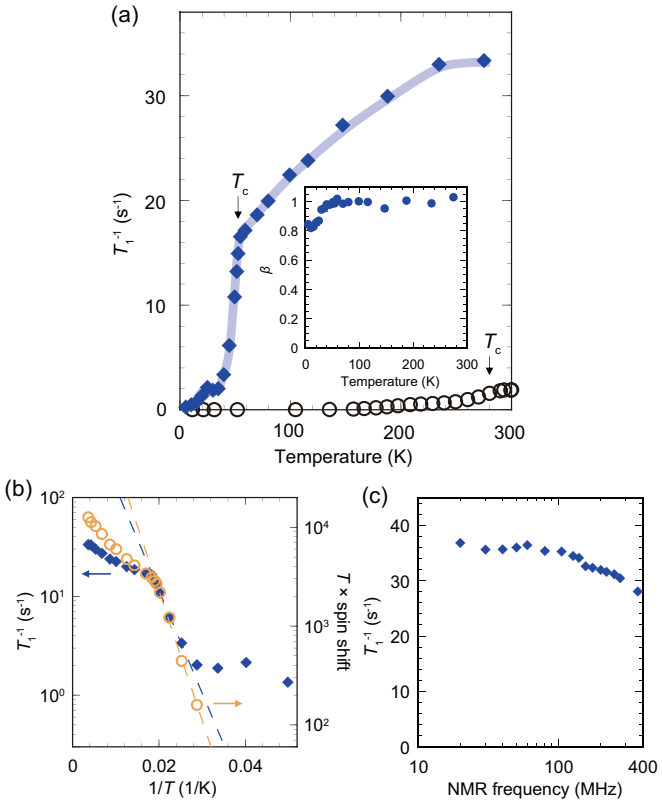

FIG. 3. (a) Temperature dependence of the ^{1}H-NMR spin-lattice relaxation rate T_1^{-1} in TTF-BA (solid blue diamonds) and TTF-CA under 13 kbar (open black circles) reported in Ref. [10]. Inset: Temperature dependence of the exponent β in the stretched exponential fitting of the nuclear relaxation curves for TTF-BA. (b) Activation plots of T_1^{-1} (solid blue diamonds) and spin shift multiplied by T (open yellow circles) in TTF-BA. The broken lines indicate single exponential fits to the data in 35 K $< T <$ T_c. (c) Frequency dependence of T_1^{-1} at 280 K in TTF-BA.

B. Spin-lattice relaxation rate T_1^{-1}

The nonmagnetic transition was also captured by a steep decrease in the spin-lattice relaxation rate T_1^{-1} below T_c [Fig. 3(a)]. The drop of T_1^{-1} just below T_c is characterized by an activation energy $\Delta_{T_1^{-1}}$ of 240 K, which is comparable with the activation value Δ_s, 300 K, characterizing the drop in the spin shift multiplied by T just below T_c, as shown in Fig. 3(b). A leveling-off in T_1^{-1} below 35 K is likely caused by free spins failing to form singlets and/or minor impurity spins, as often observed in ^{1}H-NMR for spin-singlet phases [15]; the exponent in the stretched exponential fitting of the nuclear relaxation curve, which is nearly unity above 35 K, decreases to 0.8 at 15 K [inset of Fig. 3(a)], also suggesting inhomogeneous nuclear relaxations by the dispersed orphan spins. The near agreement between the $\Delta_{T_1^{-1}}$ and Δ_s values is consistent with the singlet-triplet excitations unlike in the ferroelectric phase of TTF-CA showing a clear disagreement, which indicates that polaron excitations inheriting charge solitons vitally excited above T_c and singlet-triplet excitations occur in different energy scales and contribute to the shift and T_1^{-1} with distinct weights [12]. The contrasting behaviors of TTF-CA and TTF-BA are reasonable because TTF-CA is situated near the NI phase boundary with the charge-transfer instability, whereas TTF-BA is an ionic Mott insulator with a large charge gap of ∼8000 K [16], thus carrying low-energy excitations only in the spin degrees of freedom.

In the paramagnetic phase above T_c, the spin susceptibility and T_1^{-1} are much larger than those of TTF-CA under pressure [Figs. 2(b) and 3(a)], implying that TTF-BA is regarded as an $S = 1/2$ localized spin system, not a soliton matter as in the ionic paraelectric phase of TTF-CA [10]. This picture is supported by the frequency-insensitive T_1^{-1} observed at 280 K [Fig. 3(c)], which is compared to the pronounced frequency dependence of T_1^{-1} pointing to the diffusive motion of spin solitons [10]. We note that, in 1D Heisenberg spin systems for the high-temperature limit, T_1^{-1} is also expected to show the frequency dependence due to the classical spin diffusion [17,18]; thus, T_1^{-1} insensitive to frequency implies that TTF-BA cannot be regarded as the pure 1D spin system, which is discussed in more detail below, although the slight decrease of T_1^{-1} at higher frequencies is possibly derived from the weak 1D nature of the spin chain.

C. Evaluations of exchange interactions

The lattice structure of TTF-BA is rather complicated as seen in Fig. 1(c), where the 1D chains running along the a and b axes stack alternatively along the c direction with short TTF-TTF intercolumn contacts, quite different from TTF-CA where the 1D chains are arranged in parallel to each other [19]. We evaluated intermolecular transfer integrals in TTF-BA through molecular orbital calculations [13]. The largest transfer integral is $t_{\parallel} = 43$–46 meV between the TTF-HOMO (highest occupied molecular orbital) and the BA-LUMO (lowest unoccupied molecular orbital) along the a or b axis [the bold lines in Fig. 4(a)], the next largest one is $t_{\perp} = 28$ meV between the TTF-HOMOs along the c direction [the double lines in Fig. 4(a)], and the third largest one is $t'_{\perp} = 19$ meV between the TTF-HOMO in the $\alpha(\beta)$ chain and the CA-LUMO in the $\beta(\alpha)$ chain [the single lines in Fig. 4(a)]. Other values, for instance, the transfer integrals between the adjacent $\alpha(\beta)$ columns in parallel [the dotted lines in Fig. 4(a)], are below ∼10 meV.

For modeling the spin network of TTF-BA, we calculated the exchange interaction J between the localized spins using the two expressions derived within the second-order perturbation in the ionic Hubbard model [20]: $J = 2t^2/(U - \Delta) + 2t^2/(U + \Delta)$ for a donor-acceptor pair and $J = 4t^2/U$ for a donor-donor (acceptor-acceptor) pair, where Δ is the effective energy difference between the TTF-HOMO and BA-LUMO levels including the intersite Coulomb energy and U is the on-site Coulomb energy. In this model, the charge transfer gap is expressed by $U - \Delta$, which is 0.8 eV according to the infrared [5] and resistivity [16] measurements. With $U = 1.5$ eV employed in the theoretical calculations [21], we obtained $\Delta =$ 0.7 eV, which yields $J_{\parallel} \equiv J_{\mathrm{TTF}(\alpha)-\mathrm{BA}(\alpha)}$ (or $J_{\mathrm{TTF}(\beta)-\mathrm{BA}(\beta)}$) = 73–84 K, $J_{\perp} \equiv J_{\mathrm{TTF}(\alpha)-\mathrm{TTF}(\beta)} = 24$ K, and $J'_{\perp} \equiv J_{\mathrm{TTF}(\alpha)-\mathrm{BA}(\beta)}$ (or $J_{\mathrm{TTF}(\beta)-\mathrm{BA}(\alpha)}$) = 14 K [Fig. 4(a)]. Bewick and Soos computed $t_{\parallel} = 60$ meV based on the semiempirical theory [22], which leads to $J_{\parallel} = 140$ K, not far from the above calculation.

On the other hand, the exchange interactions can be evaluated from the experimental data of T_1^{-1} using the following

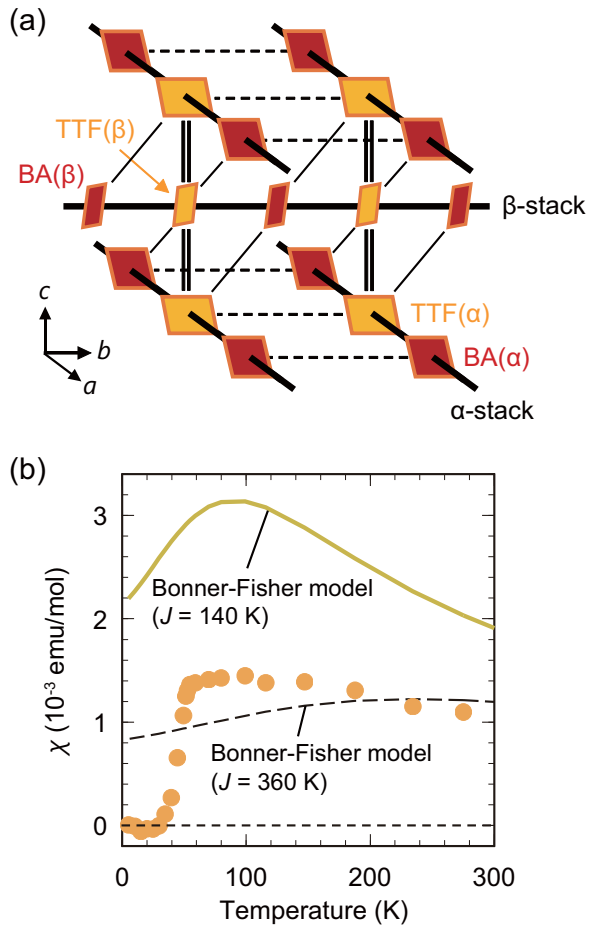

FIG. 4. (a) Network of transfer integrals (or the exchange interactions) in TTF-BA above T_c. The bold, double, and single lines represent the nearest ($t_\parallel$, $J_\parallel$), second-nearest ($t_\perp$, $J_\perp$), and third-nearest ($t'_\perp$, $J'_\perp$) neighboring molecular pairs, respectively. (b) Comparison between the experimental spin susceptibility and the Bonner-Fisher model calculations for $J = 140$ K (experimentally determined) and $J = 360$ K (for reference).

formula for localized spins in the high-temperature limit [23],

$$T_1^{-1} = \sqrt{\frac{\pi S(S+1)}{3Z}}\frac{g^2\hbar\gamma_N^2 a_\perp^2}{J}, \tag{1}$$

where Z is the number of the neighboring sites, g is the electron g-factor, γ_N is the nuclear gyromagnetic ratio, $\hbar$ is the reduced Planck constant, and $a_\perp$ is the hyperfine coupling component perpendicular to the field direction given by

$$a_\perp^2 = \frac{1}{2}\left[\left(a_{yy}^2 + a_{zz}^2\right)H_x^2 + \left(a_{zz}^2 + a_{xx}^2\right)H_y^2 + \left(a_{xx}^2 + a_{yy}^2\right)H_z^2\right], \tag{2}$$

where a_{ii} ($i = x$, y, and z) is the principal value of the hyperfine coupling tensor and H_i is the direction cosine of the applied field for the respective ^{1}H sites. In calculating $a_\perp$, we employed the a^{iso} value of -0.52 kOe/μ_B as the isotropic part and calculated the anisotropic dipole part from the on-molecular spin, which yields ($-0.3a^{aniso}$, $-1.7a^{aniso}$, $2a^{aniso}$) with $a^{aniso} \sim 0.27$ kOe/μ_B in principal values. The principal axes of the hyperfine tensor differ among the four ^{1}H sites so that H_i depends on the ^{1}H site. The average of $a_\perp^2$ over the four ^{1}H sites yields $(a_\perp^2)^{ave} \sim 0.44$ kOe$^2/\mu_B^2$ for the present field configuration of $H \parallel b^*$. Considering the interchain exchange interaction, we replace J to $\sqrt{J_\parallel^2 + J_\perp^2 + J_\perp'^2}$ in Eq. (1) with $J_\parallel = 3$–$6J_\perp = 5$–$10J'_\perp$ and $Z = 2$. The high-temperature limit of T_1^{-1} is estimated at 41 s^{-1} by extrapolating it to $1/T = 0$ in Fig. 3(b). Substituting these values in Eq. (1), we obtained $J_\parallel \sim 140$ K, which is nearly in agreement with $J_\parallel = 73$–140 K calculated from the second-order perturbation formulas.

IV. DISCUSSION

Anomalous spin excitations in TTF-BA are highlighted by comparing the spin susceptibilities derived from the spin shifts with the Bonner-Fisher curve expected in 1D antiferromagnetic (AF) Heisenberg spin systems [24,25] with $J = 140$ K obtained above. Bewick *et al.* calculated the spin susceptibility in the 1D mixed-stack charge-transfer systems described by the Peierls-Hubbard model [26], the temperature profile of which is close to the Bonner-Fisher curve for the ionic limit ($\rho \to 1$). However, on the basis of the experimentally determined J value, a large difference between the experimental data and the Bonner-Fisher curve is evident in TTF-BA with $\rho \sim 0.95$. We note that, for any J value, the Bonner-Fisher curve does not reproduce the experimental susceptibility as reported in Refs. [5,6] and shown in Fig. 4(b) [27].

In general, the spin susceptibility is more and more reduced as the number of the neighboring sites increases, and thus the complicated spin network in TTF-BA appears responsible for the reduction of the susceptibility from that of the pure 1D spin chain. However, around temperatures of $\sim J_\parallel$ and below, the intrachain AF correlations are developed so that, on a site in adjacent chains, the exchange fields produced through $J_\perp$ and $J'_\perp$ [see Fig. 4(a)] are canceled by each other due to the frustration between $J_\perp$ and $J'_\perp$. Thus, the spin network is expected to become 1D-like below $\sim$140 K; then, the remarkable discrepancy between the experimental and calculated behaviors in TTF-BA invokes unusual mechanisms of spin excitations.

We discuss the origins of the discrepancy in the light of the distinctive nature of TTF-BA as a localized spin system. The first one is the enhanced spin-lattice coupling. Theoretically, working with the semiclassical treatment of a bosonized Hamiltonian for NI transition systems, Tsuchizu *et al.* suggested that the spin susceptibility in the 1D AF Heisenberg spin systems with spin-lattice couplings and site-alternating potentials does not follow the Bonner-Fisher curve but carries unconventional excitations, called "spin polarons", unlike the conventional spinon excitations [28]. In particular, the spin-lattice coupling is expected to cause the local spin-singlet pairings even above T_c through the lattice fluctuations. Another exclusive feature of the present spin system is electric polarizability leading to polar fluctuations inherent in the mixed-stack ionic Mott insulator. Kagawa *et al.* reported that the conventional relationships Δ vs T_c and H vs T_c in spin-Peierls systems are broken in TTF-BA [6]; typically, $\Delta/k_BT_c = 2.5$ [29] and $\alpha = 0.38$ [30] in the spin-Peierls systems, whereas $\Delta/k_BT_c = 4.3$ and $\alpha = 0.18$ in TTF-BA, where α is the coefficient given by

$1 - T_c(H)/T_c(0) = \alpha[g\mu_B H/2k_B T_c(0)]^2$. The large $\Delta/k_B T_c$ value suggesting the spin gap far exceeding the energy scale of the transition and the small α value signifying outstanding robustness to magnetic field invoke an additional mechanism to stabilize the nonmagnetic phase beyond the conventional spin-Peierls framework. Polar fluctuations, which cause local donor-acceptor pairing, possibly favor precursory singlet formation in the paramagnetic phase, suppressing spin susceptibility above T_c. The frequency-dependent dielectric constant above T_c reported in Ref. [16] is possibly related to the present scenario.

We note that the behavior of the spin susceptibility in TTF-BA resembles that of the inorganic spin-Peierls material $CuGeO_3$ [31], in which its behavior can be quantitatively explained considering the next-nearest-neighbor (NNN) AF interaction in the spin chain [32]. In the present case of TTF-BA, however, the NNN interaction in the spin chain is vanishingly small due to the lack of the efficient path between the NNN sites, unlike the superexchange path in $CuGeO_3$, and thus it is unlikely that the NNN interaction is the origin of the suppression of the spin susceptibility in TTF-BA.

It is a highly likely view that the precursory singlet fluctuations observed in TTF-BA manifest themselves in an extreme manner as a dimer liquid in TTF-CA, where most of the TTF and CA molecules form polar singlet pairs, whose long-range order is interrupted by soliton excitations. TTF-BA with a charge transfer of $\rho \sim 0.95$ is a nearly perfect ionic ferroelectric, whereas TTF-CA with $\rho \sim 0.6$–0.7 is an intermediately charge-transferred electronic ferroelectric. It is intriguing to see how the donor-acceptor spin chain system varies its magnetic excitations from the local spin regime to the soliton regime when ρ is reduced from unity.

V. CONCLUSION

In conclusion, ^{1}H-NMR spectroscopy of the alternating donor-acceptor ionic chain system TTF-BA revealed that it hosts an extraordinary spin system, understandable by neither the soliton matter realized in the analogous system TTF-CA nor the conventional Heisenberg spin system with the spin-Peierls instability. The spin shift and the nuclear spin-lattice relaxation rate clearly captured the spin-singlet transition at 53 K. The paramagnetic state above 53 K is demonstrated to host localized spin chains. However, the analyses of the spin shift and T_1^{-1} found a substantial reduction in the spin susceptibility from that expected for the antiferromagnetic Heisenberg spin chains, evoking a view that TTF-BA offers an exclusive ionic spin system with unusually coupled magnetic and polar fluctuations enhanced prior to a nonmagnetic ferroelectric order. This potentially distinct cross-correlated fluctuation, which is possibly a generic feature for extensive ionic spin systems, is a profound addition to the correlated electron physics, awaiting theoretical challenges to treat jointly spin dynamics and electric polar correlation.

ACKNOWLEDGMENTS

This work was supported by the JSPS Grant-in-Aids for Scientific Research (Grants No. JP17K05532, No. JP18H05225, and No. JP19H01846) and by the Murata Science Foundation.

[1] R. E. Peierls, *Quantum Theory of Solids* (Clarendon, Oxford, 1955).

[2] M. C. Cross and D. S. Fisher, A new theory of the spin-Peierls transition with special relevance to the experiments on TTFCuBDT, Phys. Rev. B **19**, 402 (1979).

[3] J. B. Torrance, J. E. Vazquez, J. J. Mayerle, and V. Y. Lee, Discovery of a Neutral-to-Ionic Phase Transition in Organic Materials, Phys. Rev. Lett. **46**, 253 (1981).

[4] J. B. Torrance, A. Girlando, J. J. Mayerle, J. I. Crowley, V. Y. Lee, P. Batail, and S. J. LaPlaca, Anomalous Nature of Neutral-to-Ionic Phase Transition in Tetrathiafulvalene-Chloranil, Phys. Rev. Lett. **47**, 1747 (1981).

[5] A. Girlando, C. Pecile, and J. B. Torrance, A key to understanding ionic mixed stacked organic solids: Tetrathiafulvalene-bromanil (TTF-BA), Solid State Commun. **54**, 753 (1985).

[6] F. Kagawa, S. Horiuchi, M. Tokunaga, J. Fujioka, and Y. Tokura, Ferroelectricity in a one-dimensional organic quantum magnet, Nat. Phys. **6**, 169 (2010).

[7] P. García, S. Dahaoui, P. Fertey, E. Wenger, and C. Lecomte, Crystallographic investigation of temperature-induced phase transition of the tetrathiafulvalene-*p*-bromanil, TTF-BA charge transfer complex, Phys. Rev. B **72**, 104115 (2005).

[8] M. Buron-Le Cointe, E. Collet, B. Toudic, P. Czarnecki, and H. Cailleau, Back to the structural and dynamical properties of neutral-ionic phase transitions, Crystals **7**, 285 (2017).

[9] R. Takehara, K. Sunami, F. Iwase, M. Hosoda, K. Miyagawa, T. Miyamoto, H. Okamoto, and K. Kanoda, Revisited phase diagram on charge instability and lattice symmetry breaking in the organic ferroelectric TTF-QCl_4, Phys. Rev. B **98**, 054103 (2018).

[10] K. Sunami, T. Nishikawa, K. Miyagawa, S. Horiuchi, R. Kato, T. Miyamoto, H. Okamoto, and K. Kanoda, Evidence for solitonic spin excitations from a charge-lattice-coupled ferroelectric order, Sci. Adv. **4**, eaau7725 (2018).

[11] R. Takehara, K. Sunami, K. Miyagawa, T. Miyamoto, H. Okamoto, S. Horiuchi, R. Kato, and K. Kanoda, Topological charge transport by mobile dielectric-ferroelectric domain walls, Sci. Adv. **5**, eaax8720 (2019).

[12] K. Sunami, R. Takehara, A. Katougi, K. Miyagawa, S. Horiuchi, R. Kato, T. Miyamoto, H. Okamoto, and K. Kanoda, Fate of a soliton matter upon symmetry-breaking ferroelectric order, arXiv:2008.09337.

[13] T. Mori, A. Kobayashi, Y. Sasaki, H. Kobayashi, G. Saito, and H. Inokuchi, The intermolecular interaction of tetrathiafulvalene and bis(ethylenedithio)tetrathiafulvalene in organic metals. Calculation of orbital overlaps and models of energy-band structures, Bull. Chem. Soc. Jpn. **57**, 627 (1984).

[14] F. Devreux, C. Jeandey, M. Nechtschein, J. M. Fabre, and L. Giral, Electron-proton couplings and local susceptibilities in TTF and TCNQ salts, J. Phys. Fr. **40**, 671 (1979).

[15] T. Itou, A. Oyamada, S. Maegawa, K. Kubo, H. M. Yamamoto, and R. Kato, Superconductivity on the border of a spin-gapped Mott insulator: NMR studies of the quasi-two-dimensional organic system $EtMe_3P[Pd(dmit)_2]_2$, Phys. Rev. B **79**, 174517 (2009).

[16] Y. Tokura, S. Koshihara, Y. Iwasa, H. Okamoto, T. Komatsu, T. Koda, N. Iwasawa, and G. Saito, Domain-Wall Dynamics in Organic Charge-Transfer Compounds with One-Dimensional Ferroelectricity, Phys. Rev. Lett. **63**, 2405 (1989).

[17] J. Kikuchi, N. Kurata, K. Motoya, T. Yamauchi, and Y. Ueda, Spin diffusion in the $S = 1/2$ quasi one-dimensional antiferromagnet α-$VO(PO_3)_2$ via ^{31}P NMR, J. Phys. Soc. Jpn. **70**, 2765 (2001).

[18] F. Borsa and M. Mali, Experimental study of high-temperature spin dynamics in one-dimensional Heisenberg paramagnets, Phys. Rev. B **9**, 2215 (1974).

[19] J. J. Mayerle, J. B. Torrance, and J. I. Crowley, Mixed-stack complexes of tetrathiafulvalene. The structures of the charge-transfer complexes of TTF with chloranil and fluoranil, Acta. Crystallogr., Sect. B **35**, 2988 (1979).

[20] H. Katsura, M. Sato, T. Furuta, and N. Nagaosa, Theory of the Optical Conductivity of Spin Liquid States in One-Dimensional Mott Insulators, Phys. Rev. Lett. **103**, 177402 (2009).

[21] N. Nagaosa and J. Takimoto, Theory of neutral-ionic transition in organic crystals. II. Effect of the intersite Coulomb interaction, J. Phys. Soc. Jpn. **55**, 2745 (1986).

[22] S. A. Bewick and Z. G. Soos, Spin solitons in organic charge-transfer salts, Chem. Phys. **325**, 60 (2006).

[23] T. Moriya, Nuclear magnetic relaxation in antiferromagnetics, Prog. Theor. Phys. **16**, 23 (1956); Nuclear magnetic relaxation in antiferromagnetics, II, **16**, 641 (1956).

[24] J. C. Bonner and M. E. Fisher, Linear magnetic chains with anisotropic coupling, Phys. Rev. **135**, A640 (1964).

[25] W. E. Estes, D. P. Gavel, W. E. Hatfield, and D. J. Hodgson, Magnetic and structural characterization of dibromo- and dichlorobis(thiazole)copper(II), Inorg. Chem. **17**, 1415 (1978).

[26] S. A. Bewick and Z. G. Soos, Peierls transitions in ionic organic charge-transfer crystals with spin and charge degrees of freedom, J. Phys. Chem. B **110**, 18748 (2006).

[27] The definition of J is different between Refs. [5,6] and the present paper. The former papers follow the paper by Bonner and Fisher (Ref. [24]), in which the Heisenberg Hamiltonian is described as $\mathcal{H} = 2J\Sigma \boldsymbol{S_i} \cdot \boldsymbol{S_j}$. In the present paper, we define $J = 4t^2/U$ and $\mathcal{H} = J\Sigma \boldsymbol{S_i} \cdot \boldsymbol{S_j}$ for the like-spin pair. Thus, the present J value corresponds to twice the value in Refs. [5,6].

[28] M. Tsuchiizu, H. Yoshioka, and H. Seo, Phase competition, solitons, and domain walls in neutral-ionic transition systems, J. Phys. Soc. Jpn. **85**, 104705 (2016).

[29] E. Orignac and R. Chitra, Mean-field theory of the spin-Peierls transition, Phys. Rev. B **70**, 214436 (2004).

[30] M. C. Cross, Effect of magnetic fields on a spin-Peierls transition, Phys. Rev. B **20**, 4606 (1979).

[31] M. Hase, I. Terasaki, and K. Uchinokura, Observation of the Spin-Peierls Transition in Linear Cu^{2+} (Spin-1/2) Chains in an Inorganic Compound $CuGeO_3$, Phys. Rev. Lett. **70**, 3651 (1993).

[32] J. Riera and A. Dobry, Magnetic susceptibility in the spin-Peierls system $CuGeO_3$, Phys. Rev. B **51**, 16098 (1995).